EJN European Journal of Neuroscience

FENS Federation of European Neuroscience Societies

European Journal of Neuroscience, Vol. 45, pp. 267–277, 2017 doi:10.1111/ejn.13430

COGNITIVE NEUROSCIENCE

Encoding of global visual motion in the nidopallium caudolaterale of behaving crows

Lysann Wagener and Andreas Nieder
Animal Physiology, Institute of Neurobiology, University of Tübingen, Auf der Morgenstelle 28, 72076 Tübingen, Germany

Keywords: corvid songbird, motion, NCL, single-unit recordings, vision

Edited by Doug Munoz
Received 15 April 2016, revised 25 August 2016, accepted 5 October 2016

Abstract

Songbirds possess acute vision. How higher brain centres represent basic and parameterised visual stimuli to process sensory signals according to their behavioural importance has not been studied in a systematic way. We therefore examined how carrion crows (*Corvus corone*) and their nidopallial visual neurons process global visual motion information in dynamic random-dot displays during a delayed match-to-sample (DMS) task. The behavioural data show that moderately fast motion speeds (16° of visual angle/s) result in superior direction discrimination performance. To characterise how neurons encode and maintain task-relevant visual motion information, we recorded the single-unit activity in the telencephalic association area 'nidopallium caudolaterale' (NCL) of behaving crows. The NCL is considered to be the avian analogue of the mammalian prefrontal cortex. Almost a third (28%) of randomly selected NCL neurons responded selectively to the motion direction of the sample stimulus, mostly to downward motions. Only few NCL neurons (7.5%) responded consistently to specific motion directions during the delay period. In error trials, when the crows chose the wrong motion direction, the encoding of motion direction was significantly reduced. This indicates that sensory representations of NCL neurons are relevant to the birds' behaviour. These data suggest that the corvid NCL, even though operating at the apex of the telencephalic processing hierarchy, constitutes a telencephalic site for global motion integration.

Introduction

Songbirds, such as corvids, possess acute vision. One of the fundamental visual attributes is motion. Visual motion is processed along all stages of the major visual pathways in birds (Wylie *et al.*, 2015), and reaches the telencephalic NCL via the tectofugal and the thalamofugal pathways (Kröner & Güntürkün, 1999). The tectofugal pathway is thought to be homologous to the mammalian colliculo-pulvinar-cortical pathway, whereas the thalamofugal pathway is considered to be a homologue of the geniculo-cortical pathway (Karten, 1969; Shimizu & Bowers, 1999). In the tectofugal pathway, the tectum opticum, which receives more than 90% of retinal projections, feeds into the nucleus rotundus, which in turn projects to the entopallium (formerly called *'ectostriatum'*) in the telencephalon (Benowitz & Karten, 1976; Karten & Shimizu, 1989). This pathway is dominant in birds and processes motion on all pathway stages (*tectum opticum*: Frost & DiFranco, 1976; Frost & Nakayama, 1983; Frost *et al.*, 1988; Luksch *et al.*, 2004; *N. rotundus*: Wang & Frost, 1992; Wang *et al.*, 1993; Sun & Frost, 1998; *entopallium*: Nguyen *et al.*, 2004; Xiao & Frost, 2009). In the thalamofugal pathway, on the other hand, the optic nucleus of the thalamus receives retinal input and projects to the telencephalic visual Wulst. The visual Wulst shows prominent motion-selective responses (Pettigrew, 1979; Nieder & Wagner, 1999; Baron *et al.*, 2007) and plays an important role in avian binocular vision (Nieder & Wagner, 2000, 2001a,b).

The termination zones of these visual pathways, the telencephalic entopallium (tectofugal) and the visual Wulst (thalamofugal) provide input to the 'nidopallium caudolaterale' (NCL). The NCL has been implicated in executive control functions (Güntürkün, 2005; Veit & Nieder, 2013). As a pallial associative area, the avian NCL receives not only highly processed visual information but also input from all other sensory modalities (Kröner & Güntürkün, 1999). In crows, NCL neurons represent visual (Veit *et al.*, 2014) and auditory signals (Moll & Nieder, 2015). They maintain sensory information active during working memory (Veit *et al.*, 2014) to support cognitive control functions, such as numerical categorisation (Ditz & Nieder, 2015; Nieder, 2016), unimodal and cross-modal associations (Moll & Nieder, 2015; Veit *et al.*, 2015b) and abstract rules (Veit & Nieder, 2013).

Despite its role in high-level processing, the NCL would still require representations of basic sensory features. The NCL needs to evaluate and select between incoming information in order to fulfil its role as central executive. This issue has not been examined in a systematic way. Stimuli used so far in neurophysiological studies with behaving birds were rich in sensory parameters (e.g. complex

Correspondence: Andreas Nieder, as above.
E-mail: andreas.nieder@uni-tuebingen.de

images), or simple but not parameterised (e.g. few individual colours). Thus, whether the avian NCL selectively represents visual motion as a basic visual parameter remained unknown. We first hypothesised that neurons in the NCL represent the speed and direction of visual motion to guide behavioural choices. In this study, we therefore stimulated with a pure motion stimulus (moving dynamic random-dot patterns) moving at different speeds and in different directions. Dynamic random-dot displays provide a powerful tool to assess the visual capacity of crows and their motion-sensitive neurons to global image motion. In such displays, the performance of subjects does not rely on the observation of individual dots, but rather on the temporal and spatial integration of local moving dots into a percept of global motion pattern (Williams & Sekuler, 1984; Downing & Movshon, 1989). For flying animals like crows, the interpretation of global motion is essential for locomotion and orientation in their environment.

Second, we assumed that motion signals in NCL were modulated according to behavioural relevance. Sensory signals processed according to its importance for the task at hand are no longer veridical representations of the external world, but also have to reflect the internal status of the animal. Thus, the coding of sensory stimuli can change dramatically higher up in the processing hierarchy as a function of behavioural relevance. Studies on visual motion processing have been performed in anaesthetised birds (e.g. Xiao & Frost, 2009), or awake but nonbehaving birds (Baron *et al.*, 2007). However, a closer relationship between activity of motion-sensitive neurons and motion perception can only be obtained by recording from birds engaged in a task. This also avoided possible detrimental effects of anaesthesia known to exist in the avian telencephalon (Capsius & Leppelsack, 1996; Schmidt & Konishi, 1998; George *et al.*, 2004).

In this study, we therefore recorded NCL neurons while crows performed a delayed match-to-sample task with visual motion in dynamic random-dot displays as discriminandum. Besides characterising speed- and direction-selective responses, comparison of behavioural and neuronal data enabled us to evaluate the relevance of NCL motion signals for the crows' behaviour. Given that motion signals in dot displays are widely and successfully used to study perceptual decision-making processes in monkeys (Parker & Newsome, 1998), this study may pave the way for future investigations into perceptual decision making in birds.

Methods

Subjects

Two adult (both 3 years old) hand-raised carrion crows (*Corvus corone corone*), one male (crow B) and one female (crow L), were used in this experiment. The birds were housed in social groups in an indoor aviary (length 360 cm, width 240 cm, height 300 cm; Hoffmann *et al.*, 2011). They were on a controlled feeding protocol during the training and recording period. Body weight was measured daily. The daily amount of food was given as reward during, or if necessary after, the sessions. Food was provided in the aviary on days without experimentation. Water was *ad libitum* available in the aviary and during the experiments. All procedures were carried out according to the guidelines for animal experimentation and approved by the responsible national authorities, the Regierungspräsidium Tübingen, Germany.

Experimental setup

The birds were placed on a perch in front of a touchscreen monitor (3M Microtouch, 15″, 60 Hz refresh rate) in a darkened operant conditioning chamber (length 100 cm, width 76 cm, height 100 cm). Viewing distance to the monitor was 14 cm. The behaviour was controlled by the CORTEX system (National Institute of Mental Health, MD, USA) which also stored the behavioural data. An automated feeder delivered either mealworms (*Tenebrio molitor* larvae) or bird seed pellets upon correctly completed trials. Additionally, the birds received specific auditory feedback sounds for correct and error trials. During each trial, crows were trained to keep their head still in front of the computer display. A trial only started when the crow moved its head into the beam of an infra-red light barrier and kept its head still throughout the trial, thus ensuring stable head position. This was controlled via a reflector foil attached to the crows' head. Whenever the crow made premature head movements and thereby left the infra-red light barrier with its head during an ongoing trial, the computer terminated the trial, and the trial was discarded. Neuronal data were recorded using the PLEXON system (Dallas, TX, USA).

Stimulus display

The stimuli were circular moving dynamic random-dot patterns with 16 dva (degree of visual angle) diameter. The dots were moved with 100% coherence in either of 12 directions in steps of 30°. Each dot was white and had a radius of 0.12 dva shown on black background with a density of 4 dots/dva² and a lifetime of 20 frames. The displays were generated using a custom-written MATLAB script. To determine tuning to motion speed, four different speeds (4, 8, 16 and 32 dva/s) were used in a fraction of the sessions (33 for crow B and 22 for crow L). Motion speed was not task-relevant. To determine direction-selectivity, either dot patterns moving in all four speeds were presented with equal probabilities and responses to all four speeds were combined, or dot patterns moved at 16 dva/s.

Behavioural task

The crows performed a delayed match-to-sample (DMS) task in which they discriminated the directions of moving dot stimuli (Fig. 1). The crow started a trial by positioning its head in front of the monitor whenever a go-stimulus (small white cross) was shown on the screen, thus closing an infra-red light barrier, and maintaining the head still throughout the trial. To indicate that the light barrier had been entered, the bird heard a click sound and the go-stimulus on the screen turned into a white circle for 60 ms. Next, a 200 ms pre-sample phase without any stimulus on the screen followed. After this, the sample stimulus (i.e. moving random-dot pattern) was presented for 800 ms in the centre of the screen. The direction and the speed of the moving dots were pseudo-randomly selected. The crow had to memorise the sample motion direction during the delay phase in which only the black monitor background was visible. Delay duration was 1000 ms for all trials, except for a delay duration of 1500 ms in three sessions for crow B. In the following test phase, the test1 display was shown for 800 ms. Test1 was a 'match' in 50% of the cases, i.e. it showed the same motion direction as the sample stimulus. The crow had to respond within 800 ms after test1 onset to indicate a direction match by moving its head out of the light barrier. In the other 50% of the cases, the test1 was a 'non-match' showing dots moving in a different direction from the sample display. Here, the crow had to refrain from responding and wait for 150 ms until the test2 display, which was always a direction match, appeared. For crow L, the motion direction in the test phase was always in the opposing direction relative to the sample. For

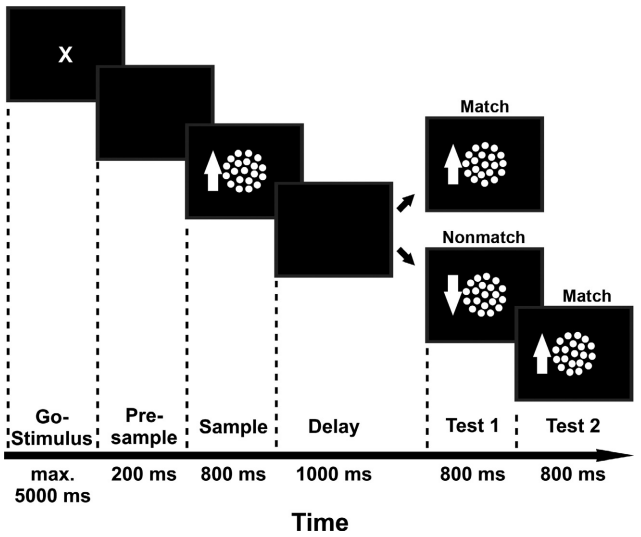

FIG. 1. Behavioural task protocol. A trial was initiated by moving the head into a light barrier. After a pre-sample phase, the sample stimulus was presented for 800 ms (white arrow indicates the motion direction of the random-dots), followed by a delay of 1000 ms. In the test phase, the match stimulus with dots moving in the same direction and at the same speed as in the sample period was shown as the first test item in 50% of the trials (match condition). In the other half of the trials, an 800 ms nonmatch stimulus with dots moving in the opposite direction preceded the match stimulus (nonmatch condition). For crow B, the direction of the nonmatch stimulus was shifted 90° clockwise to the sample direction. The bird was rewarded for responding by moving its head out of the light barrier whenever the match stimulus was presented.

crow B, the motion direction in the test phase was 90° clockwise relative to the sample (to increase discrimination performance; see Results). Note that all neuronal analyses are performed prior to test onset; the sample and delay period are therefore equal for both crows. Throughout a trial, the speed of the test stimuli was always consistent with the speed of the sample stimulus. Responses to the nonmatch stimulus and no response to either of the two test stimuli were considered as error trials and therefore not rewarded.

Both crows had participated in previous experiments and were therefore already habituated to the experimental setup. Training began with the discrimination of upward (90°) and downward (270°) motions. Once the bird reached an appropriate performance, another two directions [rightward (0°) and leftward (180°)] were introduced before the gradual addition of intermediate directions. Finally, all 12 directions were presented in a pseudo-random fashion during each session. This training procedure was identical for both birds.

Behavioural analysis

Performance to speed was tested to displays moving at speeds of 4, 8, 16 and 32 dva/s, with data combined across all 12 motion directions. The motion direction discrimination results were analysed using the data from trials with a motion speed of 16 dva/s. Two parameters were used to examine the behaviour of the birds. First, the behavioural performance, which quantifies the ratio of correct answers, was calculated as the number of correct trials divided by the total number of trials. As a second characteristic, the reaction time was defined and measured in 'match conditions' as the time from onset of the test stimulus until the bird responded by moving its head out of the light barrier.

Surgery and electrophysiological recording

The surgery was performed while the animal was under general anaesthesia with a mixture of ketamine (50 mg/kg) and Rompun (5 mg/kg xylazine). The head was placed in a stereotaxic holder (Karten & Hodos, 1967). To locate the target region, stereotaxic coordinates (centre of craniotomy: AP 5 mm, ML 13 mm) were used. Two custom-built microdrives with four glass-coated tungsten microelectrodes (2 MΩ impedance, Alpha Omega LTD, Israel) each and a connector for the head stage were chronically implanted. The eight electrodes were located at the NCL of the right hemisphere of crow B and the left hemisphere of crow L. Recordings were made over a period of several weeks across different depths of the NCL from about 1 to 6 mm below the endbrain surface. The anatomical location of the corvid NCL and the recording sites can be seen in Figs 3A and 4 of Veit & Nieder (2013), and in Fig. 3 of Veit *et al.* (2014). A small head post for the reflector of the light barrier was already implanted in the course of previous experiments. After the surgery, the bird was provided with postoperative analgesics (morphasol, 1 mg/kg butorphanol).

Each session started with adjusting the electrodes until a proper neuronal signal was detected on at least one channel. The neurons were never pre-selected for any involvement in the task. Single-cell separation was done offline (Plexon Offline Sorter, version 2.6.2). We have previously published example recording traces and action potential waveforms recorded from behaving crows (see Fig. 4, Veit & Nieder, 2013). Data analysis was performed using MATLAB (MathWorks, R2013b).

Neuronal analysis

Visual responsiveness and motion selectivity

The analysed neuronal data included cells with an average firing rate higher than 1 Hz during the entire trial and at least 10 correct trials of each sample direction (in the case of direction-selectivity analysis) and speed value (in the case of speed-selectivity analysis) respectively. To identify visually responsive units, the responses in a 300 ms window after pre-sample onset were compared with the responses of the same neuron to all motion speeds and directions in a 300 ms window shifted by 100 ms from stimulus onset (to account for response latency) applying a Wilcoxon signed-rank test ($P < 0.05$). To analyse the response selectivity to the motion speed or direction of the sample stimulus, an 800 ms time window shifted by 100 ms from stimulus onset (to account for response latency) was used. The response in the delay period was measured within a 900 ms time window at the end of the delay with 100 ms extending into the test period.

To identify direction-selectivity, defined as a difference in the firing rate as a function of motion direction (12 motion directions), a Kruskal–Wallis one-factor ANOVA was performed ($P < 0.05$). Direction-selectivity was analysed by combining the data of all motion speeds. To test whether the proportion of selective neurons is related to (or specific for) individual crows, we calculated a chi-square (χ^2) test for association of two variables (frequency and crow). The preferred direction was defined as the direction which yielded the highest firing rate, the anti-preferred direction as the direction opposite to the preferred direction. The least preferred direction was the direction to which the neuron showed the lowest firing rate. An average polar plot was generated for all direction-selective cells in the sample period, showing the activity of the population to each direction as percentage of the activity to the preferred direction. For this purpose, the firing rates of each selective neuron were aligned

with the preferred direction pointing upward and normalised by setting the response to the preferred direction as 100%.

Response latency

The response latency of a neuron was defined as the first time point at which the average firing rate of a neuron in the sample period was different from baseline activity by three standard deviations (SDs) for 10 consecutive windows. For this purpose, the firing rate of the neuron on all correct trials was averaged in 20 ms windows. The mean and SD of the baseline activity was calculated in a 250 ms time window containing the pre-sample phase and the first 50 ms after onset of the sample stimulus. The interquartile range (IQR) specified the dispersion around the median latency and was calculated as the difference between the 25th and 75th quartile.

Selectivity indices

We used two indices to characterise the strength of tuning. First, the firing rates to the preferred and anti-preferred direction or speed, respectively, were used to calculate the preferred-anti-preferred index (PAI):

$$\mathrm{PAI} = (\mathrm{FR\_pref} - \mathrm{FR\_anti\text{-}pref})/(\mathrm{FR\_pref} + \mathrm{FR\_anti\text{-}pref}),$$

where FR_pref is the cell's discharge rate to the preferred motion direction and FR_anti-pref is the firing rate to the motion direction opposite to the preferred direction. To exploit the maximum range of responses (the anti-preferred direction not always resulted in minimum activity), we also calculated the traditional minimum-versus-maximum selectivity index (SI):

$$\mathrm{SI} = (\mathrm{FR\_max} - \mathrm{FR\_min})/(\mathrm{FR\_max} + \mathrm{FR\_min}),$$

where FR_max is the cell's discharge rate to the preferred motion direction (maximum per definition) and FR_min is the firing rate to any motion direction eliciting the lowest discharge. The indices take values between 0 and 1, with values around 1 indicating strong selectivity.

Discriminability

The discriminability between the preferred and anti-preferred direction was further quantified using receiver operating characteristics (ROC) analysis. The area under the ROC curve (AUROC) was used as a measure for the overlap between the distributions of the firing rates to the preferred and to the anti-preferred direction. It could reach values between 0 and 1 (both perfect discriminability). A value of 0.5 indicated no discriminability of the preferred and the anti-preferred direction based on the firing rates to these directions.

Speed selectivity

Speed selectivity was identified by combining discharges to motion direction, using a Kruskal–Wallis one-factor ANOVA ($P < 0.05$). Neurons were included for analysis if at least 10 trials per speed value were recorded. The preferred motion speed was determined as the speed which elicited the highest firing rate. The least preferred speed was defined as the speed which led to the lowest firing rate. The average tuning functions for the population of speed-selective neurons were calculated combining the data of all neurons which were speed selective in the sample period. For this purpose, the firing rate to the preferred speed of each neuron was set 100% and the firing rate to the least preferred speed was set 0%. The normalised tuning properties were then averaged across all neurons, which preferred the same motion speed.

Time course of activity

To investigate the time course of responses, we constructed normalised and averaged spike-density histograms. For normalisation, we subtracted each cell's baseline activity, defined as 250 ms after pre-sample onset. We then normalised the firing rates to units of standard deviation from baseline (by bin-wise dividing firing rates by the standard deviation derived from baseline). Finally, single-cell normalised spike-density histograms were averaged across selective neurons. In addition, we used a sliding AUROC analysis to study the time course of discriminability averaged across selective neurons. For each neuron, AUROC values were calculated in 100 ms time windows which were advanced in steps of 10 ms. The time course of single-cell AUROC values was then averaged across selective neurons.

Error trial analyses

We performed error trial analyses with the direction-selective neurons to identify discharge differences between correct responses and mistakes. Only direction-selective neurons with at least three error trials per preferred direction were included (the number of neurons for the error trial analysis is therefore lower). First, we compared the normalised firing rates of each neuron to its preferred motion direction (i.e. 1/12 of all sample trials consisting of 12 motion directions) in correct and error trials. Because neurons show peak tuning functions, discharge rates lower than the maximum (characteristic for the preferred direction) would signal motion direction adjacent to the preferred one. If neurons do not signal their preferred motion direction, the crow might be error prone. Next, we compared the quality of discriminability between the preferred and anti-preferred direction for each cell in error relative to correct trials by deriving the AUROC values. Error AUROC values were obtained by comparing the distribution for each cell's preferred and anti-preferred direction during error trials (only cells with at least three error trials per preferred and anti-preferred direction were included). Control ROC values for correct trials were obtained by comparing the distribution for each cell's preferred and anti-preferred direction during correct trials. A decrease in the AUROC value during error trials indicates diminished discriminability between the preferred and anti-preferred directions.

Results

Behavioural performance

Two crows were trained to discriminate the motion direction of dynamic random-dot displays in a DMS task (Fig. 1). We first evaluated the crows' sensitivity to motion speed. To that aim, random-dot displays were presented in four different speeds of 4, 8, 16 and 32 dva/s, and in 12 different directions. Both crows performed above chance and showed systematically different accuracies for the four different motion speeds (Kruskal–Wallis one-factor ANOVA, $P < 0.001$, crow B: $n = 33$, crow L: $n = 22$) with best performances for motion speed of 16 dva/s (Fig. 2A and B). Crow B showed a performance of 63% (±1.0% SEM, $n = 33$ sessions) correct responses to all speeds combined (match 77%, nonmatch 54%). The number of trials per session for crow B was between 192 and 786

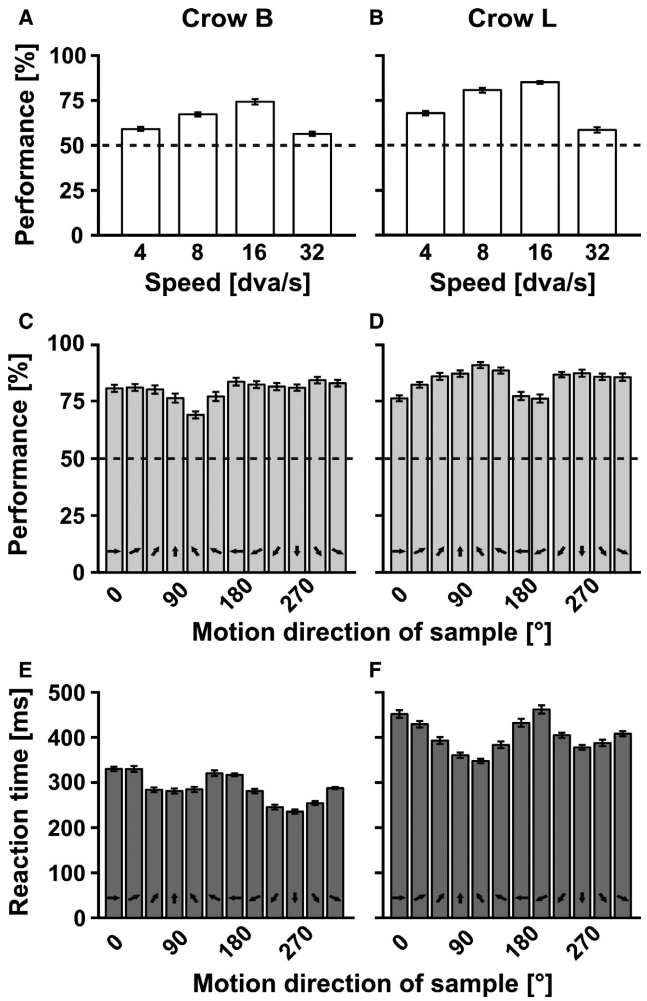

FIG. 2. Behavioural results in the direction discrimination task. (A,B) Behavioural performance depending on the motion speed of the sample stimulus for both crows. Error bars indicate SEM over the sessions (crow B: $n = 33$, crow L: $n = 22$). Dotted line indicates 50% chance level. (C,D) Average behavioural performance depending on the motion direction of the sample stimulus for both crows. Error bars indicate SEM (crow B: $n = 24$ sessions, crow L: $n = 46$ sessions). Dotted line indicates 50% chance level. (E,F) Reaction time depending on the motion direction of the sample stimulus for both crows. Error bars indicate SEM over the sessions (crow B: $n = 24$, crow L: $n = 46$).

trials. Crow L had a performance of 71% (±0.8% SEM, $n = 22$ sessions) of correct responses (match 72%, nonmatch 71%). The number of trials per session for crow L was between 272 and 671 trials.

The speed of 16 dva/s was chosen to test behavioural motion direction discrimination for the same dynamic random-dot displays moving in 12 different directions in increments of 30°. The behavioural performance of both birds was well above the 50% chance level for all sample directions (Binomial test, $P < 0.001$). On average, crow B reached 80% (±1.1% SEM, $n = 24$ sessions) of correct responses (match 97%, nonmatch 54%). The number of trials per session for crow B was between 403 and 733 trials. Crow L reached 83% (±0.5% SEM, $n = 46$ sessions) of correct responses (match 96%, nonmatch 88%). The number of trials per session for crow L was between 220 and 581 trials. Both crows showed mild performance differences depending on the motion direction of the sample stimulus (Fig. 2C and D; Kruskal–Wallis one-factor ANOVA, $P < 0.001$). Crow B performed best with sample stimuli moving down-rightward (300°) and worst for the opposite up-leftward (120°) motion direction. Crow L showed best performance for up-leftward (120°) motions and worst performance for the left-downward (210°) motion direction.

A significant effect of the motion direction on the reaction times of both birds was observed (Kruskal–Wallis one-factor ANOVA, $P < 0.001$, Fig. 2E and F). The average reaction time of crow B was 288 ± 3 ms (SEM, $n = 24$). Crow B responded fastest with 236 ± 5 ms when the direction of the sample stimulus was downward (270°), and slowest with 330 ± 5 ms for the rightward (0°) motion. The reaction times of crow L were in general slower than those of crow B (two-sample t-test, $t(68) = 20.16$, $P < 0.001$). Crow L responded on average with 401 ± 4 ms (SEM, $n = 46$). Crow L responded fastest with 348 ± 5 ms for the up-leftward (120°) motion and slowest with 462 ± 9 ms when the motion direction was left-downward (210°). A negative correlation between reaction time and behavioural performance was observed for crow L (Pearson's correlation, $n = 12$, $r = -0.93$, $P < 0.001$). The performance was best with short reaction times and worse with longer reaction times. Crow B did not show such a correlation (Pearson's correlation, $n = 12$, $r = -0.06$, $P = 0.84$).

Neuronal data

Speed selectivity

We next recorded the activity of single neurons in the NCL of the same two crows while they solved the delayed motion discrimination task. We first evaluated the selectivity of 125 NCL neurons to motion speed combined for all 12 different motion directions while the crows discriminated random-dot displays of four different speeds (4, 8, 16 and 32 dva/s). More than 60% of the tested cells (76/125) were visually responsive to sample onset. Of those, 36% (27/76) were excited and 64% (49/76) were suppressed.

A neuron was considered to be speed selective in the sample period if its firing rates (only correct trials included) to the four different motion speeds were significantly different (Kruskal–Wallis one-factor ANOVA, $P < 0.05$). Two example speed-selective neurons are shown in Fig. 3. The neuron in Fig. 3A discharged maximally to the fastest motion speed of 32 dva/s, its preferred speed. The corresponding speed tuning function (inset in Fig. 3A) increased monotonically. The example neuron in Fig. 3B preferred the intermediate speeds. A motion speed of 16 dva/s (and 8 dva/s) elicited highest responses, with a drop-off towards slower and faster speeds, thus forming a peaked tuning curve. This neuron was not only tuned to speed but also to motion direction (see Fig. 4B). The average tuning functions of all speed-selective neurons are shown in Fig. 3C. Of the 125 neurons, 19% (24/125) were significantly modulated by motion speed (Kruskal–Wallis one-factor ANOVA, $P < 0.05$). The proportions of speed-selective neurons were similar for both birds [χ^2 (1, $n = 125$) = 1.89, $P > 0.05$].

The preferred speed of each neuron was determined as the speed which resulted in the highest firing rate. The distribution of preferred speeds is depicted in Fig. 3D. Half of the speed-selective neurons (50%; 12/24) preferred the fastest speed of 32 dva/s, whereas about a third of the neurons (38%; 9/24) preferred the slowest speed of 4 dva/s. Fewer neurons (13%; 3/24) had the intermediate speed of 16 dva/s (neurons with a preferred speed of 8 dva/s were not detected). The responses to the preferred and least preferred motion speed of individual neurons were used to calculate the minimum-versus-maximum selectivity index (SI) as a measure of modulation strength. With a theoretical maximum of 1 (maximum modulation)

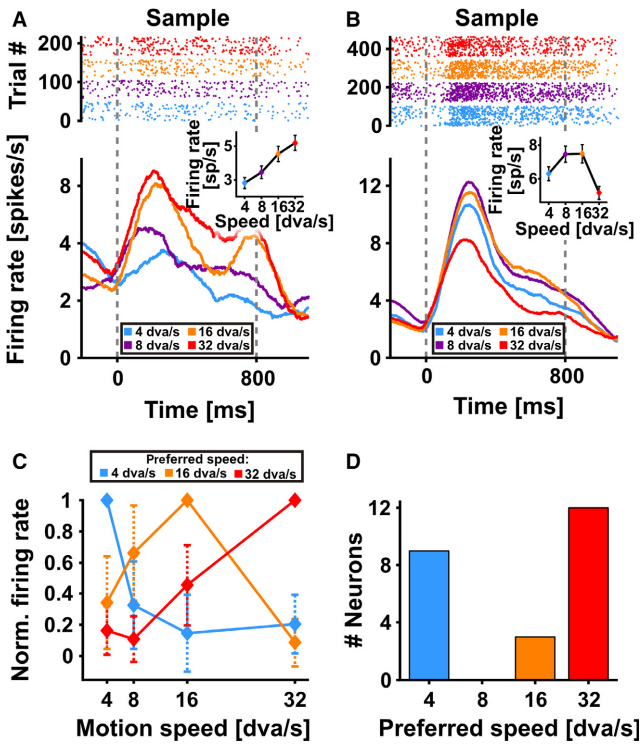

FIG. 3. Neuronal motion speed activity during sample presentation. (A,B) Activity of two speed-selective neurons in the sample period. Top displays show the dot-raster histograms with each line indicating one trial and each dot representing an action potential. Bottom displays show the corresponding spike density functions, representing the time course of the average response to each motion speed (smoothed by a 300 ms Gauss kernel). Conditions in the dot-raster histograms and the spike-density histograms show corresponding colour. Vertical dotted lines separate the different periods of a trial by indicating onset and offset of the sample stimulus. Tuning function insets show the average firing rate of the neuron to each motion speed. Error bars indicate SEM over all trials for each motion speed. (C) Average tuning functions for neurons preferring the same motion speed in the sample period. Error bars indicate SD over the neurons. (D) Frequency distribution of the neurons' preferred motion speeds. [Colour figure can be viewed at wileyonlinelibrary.com].

and a minimum of 0 (no modulation), NCL cells reached an average speed SI value of 0.29.

Direction selectivity

A total of 146 NCL neurons (44 from crow B and 102 from crow L) were tested for motion direction selectivity. Of all 146 cells, 64% (93/146) were visually responsive to sample onset. Of those, 37% (34/93) were excited and 63% (59/93) were suppressed. A neuron was considered to be directionally selective in the sample period if its firing rates (only correct trials included) to the different motion directions were significantly different (Kruskal–Wallis one-factor ANOVA, $P < 0.05$). The responses of two selective example neurons to the 12 different motion directions are shown in Fig. 4. These neurons showed maximum discharge to their preferred directions down-rightward (300°; Fig. 4A), and leftward (180°; Fig. 4B). The proportions of directional selective neurons in the sample period were similar for both birds ($\chi^2(1, n = 146) = 2.14$, $P > 0.05$) and constituted 28% of all cells recorded from the two birds (41/146). Their median response latency, which could be determined for 19 of the 41 direction-selective neurons, was 112 ms (IQR: 46.8 ms).

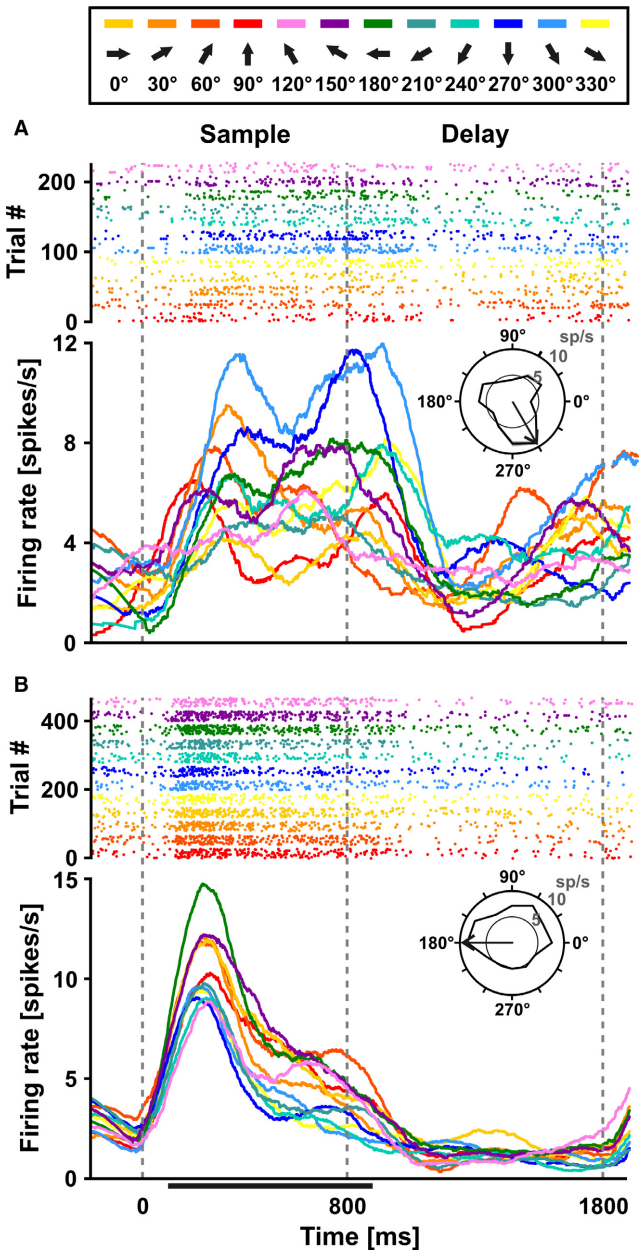

FIG. 4. Neuronal motion direction activity during sample presentation. (A,B) Activity of two direction-selective example neurons. Both neurons were selective in the sample phase (the black line along the timeline indicates the analysed time window). Layout for dot-raster histograms and spike-density functions as in Fig. 3A and B. Polar plot insets depict the direction tuning in the sample phase. Solid line indicates the average firing rate to each direction. Shadow shows SEM over the trials. The arrow indicates the preferred direction during the sample. [Colour figure can be viewed at wileyonlinelibrary.com].

The preferred direction of each selective neuron was determined as the direction which resulted in the highest firing rate. Almost all preferred directions were represented, but neurons preferring downward (270°) motion were most frequent (Fig. 5A). No evidence for clustering of neurons preferring the same or similar directions was found. The average response of the entire population of direction-selective neurons to each direction relative to the preferred one is shown in the polar plot in Fig. 5B, with the firing rate to the preferred direction of each neuron aligned pointing upward. Next to the preferred direction, the immediately adjacent directions (±30° relative to the preferred direction) showed the next highest

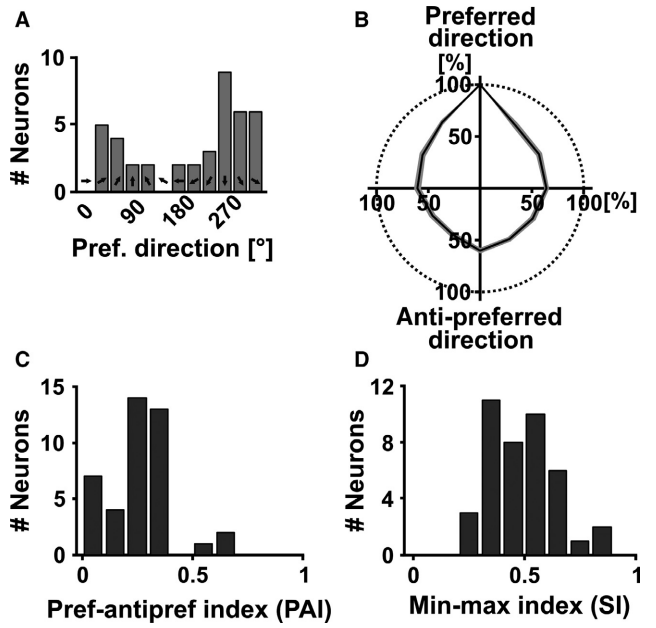

FIG. 5. Characteristics of motion direction-selectivity in the sample period. (A) Frequency distribution of the neurons' preferred directions. (B) Direction tuning during sample presentation. Average firing rates are specified as percentage of the response to the preferred direction. The polar plot is aligned with the preferred direction pointing upward. Dotted circle indicates percentage of the firing rate to the preferred direction (100% by definition). Shadow shows the SEM over the neurons (n = 41). (C) Frequency distribution of preferred-anti-preferred selectivity indices (PAI). (D) Frequency distribution of minimum-versus-maximum selectivity indices (SI).

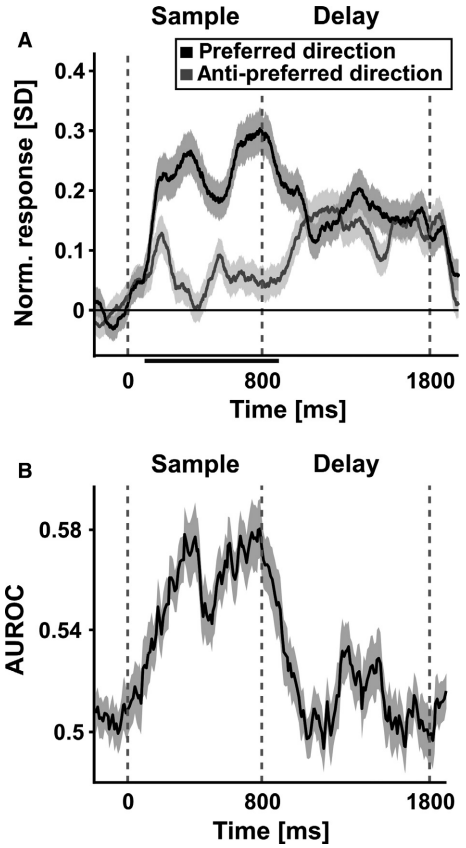

FIG. 6. Time course of responses of direction-selective neurons. (A) Average time course of the baseline-normalised responses to the preferred and anti-preferred direction. Spike density curves were smoothed by a 100 ms Gauss kernel. The black curve indicates the response to the preferred direction, the grey curve shows the response to the anti-preferred direction. Shadows show SEM over the neurons (n = 41). Vertical dotted lines separate the different periods of a trial by indicating onset and offset of sample and delay respectively. The black line along the timeline indicates the analysed time window. (B) Time course of the sliding ROC analysis, indicating the discriminability between the preferred and anti-preferred direction based on the corresponding firing rates. Shadow shows SEM over the neurons (n = 41).

discharge rates. The activity to the anti-preferred direction was at 60 ± 3% (SEM, n = 41) of the firing rate to the preferred direction. However, the anti-preferred direction did not elicit the lowest activity, but the direction shifted 30° clockwise to the anti-preferred direction (52 ± 3% SEM, Wilcoxon signed-rank test, n = 41, $P < 0.05$).

We therefore used two slightly different indices to quantify the directional selectivity. The responses to the preferred and anti-preferred motion directions of individual neurons were used to calculate the preferred-anti-preferred index (PAI) as a measure of tuning strength. With a theoretical maximum of 1 (maximum selectivity) and a minimum of 0 (no selectivity), the average PAI value of the NCL cells that were significantly tuned to direction was 0.26 ± 0.02 (SEM, n = 41; Fig. 5C). In addition, we calculated the traditional minimum-versus-maximum selectivity index (SI) using the preferred and least preferred direction. Compared to the PAI, the SI resulted in significantly higher values of 0.48 ± 0.14 (SEM, n = 41; Wilcoxon signed-rank test, n = 41, $P < 0.001$; Fig. 5D).

Next, we investigated the time course of motion selectivity. To that aim, we first calculated the average baseline-normalised spike-density histogram of the entire population of direction-selective neurons. The normalised population histogram for the neurons' preferred and anti-preferred directions can be seen in Fig. 6A. The response to the anti-preferred direction was significantly lower than to the preferred direction (Wilcoxon signed-rank test, n = 41, $P < 0.01$). In addition, we calculated the time course of directional discriminability. The discriminability between the preferred and anti-preferred direction was measured using AUROC values (area under the ROC curve). As plotted in Fig. 6B, AUROC values increased relative to the no discriminability value of 0.5 (pre-sample phase) shortly after sample onset to remain elevated. The population of directional selective neurons was therefore able to discriminate preferred from anti-preferred motion direction throughout the sample period.

Finally, direction selectivity in the delay period was examined. Only 7.5% of the neurons (11/146) responded selectively to particular directions (Kruskal–Wallis one-factor ANOVA, $P < 0.05$), which was close to chance level. To test if motion direction selectivity might occur only during brief time epochs, we ran the analysis also for shorter time windows (Zaksas & Pasternak, 2006). A 150 ms window was slid along the spike train in 75 ms increments for the entire duration of the delay (1000 ms). A neuron was classified as direction selective if at least 150 ms of activity were different according to the direction of the sample stimulus ($P < 0.0045$, Kruskal–Wallis one-factor ANOVA with Bonferroni correction). This procedure was repeated with a 300 ms window and 150 ms increments. This approach resulted in even fewer significant cells (five neurons with the 150 ms window, and nine neurons with the 300 ms window). Motion direction signals during the delay period were largely absent.

Comparison of directional signals during correct and error trials

To gain information about the behavioural relevance of the recorded neurons, we compared directional discharges to the preferred

direction of each neuron during correct and error trials. If the maximal discharges of tuned neurons to their respective preferred directions guide the crows' behavioural performance, we expect that less than maximal firing rates are correlated with direction discrimination errors. This is because less than maximal firing rates would signal motion direction adjacent to the preferred one. To that aim, we compared the absolute firing rates to the preferred motion direction of each neuron in correct and error trials. In error trials, the firing rate to the preferred direction during the stimulus presentation was decreased by 24% from 5.0 to 3.8 Hz, on average (Wilcoxon signed-rank test, $n = 33$, $P < 0.001$). Figure 7A shows the time course of the baseline-normalised and averaged responses of the population of neurons to their respective preferred motion direction in correct and error trials. Direction-selective signals were dramatically decreased during error trials.

In addition, we quantified the discriminability between the preferred and anti-preferred direction by calculating the AUROC values based on each cell's firing rate distributions to the preferred vs. anti-preferred direction in correct and error trials. The median AUROC value for sample-selective neurons was 0.67 in correct trials and 0.51 in error trials, and thus significantly decreased in error trials (Wilcoxon signed-rank test, $n = 28$, $P < 0.01$, Fig. 7B). The reduction in discriminability during error trials was even more pronounced between preferred and least preferred direction (median AUROC value in correct trials and error trials was 0.77 and 0.58 respectively; Wilcoxon signed-rank test, $P < 0.001$). The reduced activity to the preferred motion direction during error trials suggests that NCL activity provides behaviourally relevant signals rather than a veridical representation of the physical motion properties.

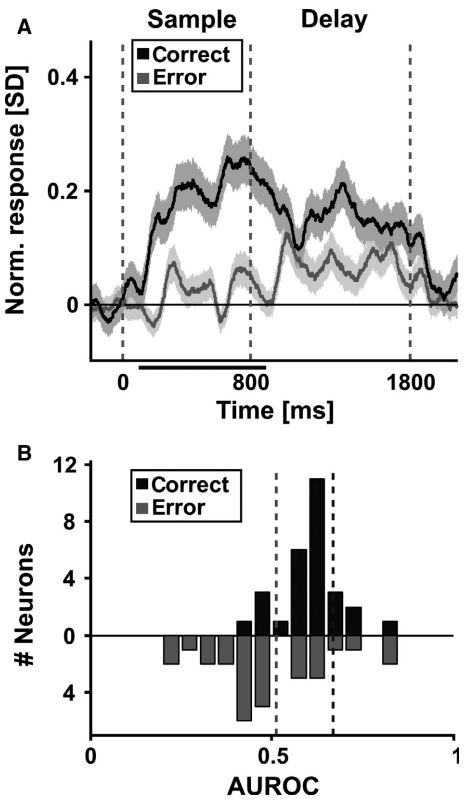

FIG. 7. Comparison of motion direction signals in correct and error trials. (A) Average response to the preferred direction of neurons with direction-selectivity in the sample period ($n = 33$). Spike density curves are smoothed by a 100 ms Gauss kernel. The dark grey curve indicates the response to the preferred direction in correct trials, the light grey curve shows the response to the preferred direction in error trials. Shadows show SEM over the neurons. Vertical dotted lines separate the different periods of a trial by indicating onset and offset of sample and delay respectively. The black line along the timeline indicates the analysed time window. (B) AUROC values quantifying the discriminability of the preferred and anti-preferred direction in correct and error trials for direction-selective neurons ($n = 28$). Vertical dotted lines indicate the median AUROC value in correct trials (dark grey) and error trials (light grey).

Discussion

This study presents behavioural and neuronal correlates of global visual motion representations in crows, corvid songbirds. We found that direction-selective activity, common along various processing stages of the tectofugal and thalamofugal visual pathways of birds, was also present in NCL neurons. Motion direction selectivity in NCL was not a mere representation of physical stimulus parameters, but related to task performance.

Behavioural motion discrimination

Both crows discriminated motion direction in random-dot displays proficiently (80 and 83%, on average), and showed performances similar to those in a delayed match-to-sample task with complex images (82 and 93%; Veit *et al.*, 2014) or numerosities (between 74 and 80%; Ditz & Nieder, 2015, 2016) as discriminanda. Slight differences in the performance according to the motion direction of the sample stimulus were observed that were, however, not consistent between the crows and could not be related to training effects. Training began with the discrimination of upward and downward motions before leftward and rightward motions, and finally, the intermediate directions were gradually introduced. However, the birds did not perform best for these initial, and thus, more familiar directions. Rather, intermediate directions led to the best performance. We assume these differences in performances and reaction times to reflect individual differences rather than specifics of the avian motion processing system.

The crows were well able to discriminate motion directions with speeds of 8 and 16 dva/s, but had problems with slower and faster moving dots. Qualitatively, similar findings have been made in pigeons, for which the lower speed threshold (75% performance criterion) with moving bars were around 5 deg/s (Hodos *et al.*, 1975) and with dynamic random-dot stimuli even 28 deg/s (Bischof *et al.*, 1999). Besides speed thresholds, also motion coherence thresholds (for random-dot stimuli) were much higher for pigeons than for humans (Bischof *et al.*, 1999). Together with similar findings in other studies (Hodos *et al.*, 1975; Mulvanny, 1978), this suggests an increased threshold for detecting motion in pigeons relative to humans. It is important to note, however, that many birds process stimuli that are displayed in the frontal or lateral visual fields differently, with the lateral visual field being more sensitive to visual motion (Martinoya *et al.*, 1983). Pigeons and songbirds seem to be severely limited in perceiving slow motion, particularly in the frontal visual field.

Role of NCL in global motion integration

Almost a third of the NCL neurons (28%) were found to respond selectively to the motion direction in dynamic random-dot stimuli. Motion responses in NCL are consistent with the visual input it receives from both the thalamofugal (via the visual Wulst) and

tectofugal (via the entopallium) pathway. As pre-synaptic areas feeding into the nidopallium seem to largely lack motion integration, the NCL may constitute a telencephalic site for global motion integration.

The visual Wulst of the thalamofugal pathway contains up to 90% of direction-selective neurons (Wagner & Frost, 1994; Nieder & Wagner, 1999; Baron *et al.*, 2007; Ng *et al.*, 2010), but global motion integration is lacking. Baron *et al.* (2007) examined the responses of owl Wulst neurons to plaid stimuli consisting of two overlapping component gratings moving in two different directions spaced 90° apart. Perceptually, the two-component motion directions are integrated to give rise to the perception of a single pattern moving in the intermediate direction. In the visual Wulst of owls, the majority of direction-selective neurons respond to the motion direction of the motion component in plaid stimuli, not the overall pattern motion. The authors therefore suggested that motion integration might emerge upstream in the telencephalon (Baron *et al.*, 2007).

Neurons in the caudal entopallium of the tectofugal pathway are tuned to the direction of visual motion as well (Engelage & Bischof, 1996; Gu *et al.*, 2002). When Nguyen *et al.* (2004) performed a lesion study in behaviourally trained pigeons, they not only found evidence for an involvement of the entopallium in motion integration but also a segregation of motion and form processing streams. They contrasted motion perception using dynamic random-dot stimuli with spatial-pattern perception for square wave gratings. They found that lesions of the caudal entopallium impaired performance on a visual motion but not a spatial-pattern task. In contrast, lesions of the rostral entopallium impaired performance on a spatial-pattern task but not the visual motion task. Thus, a separation of visual motion and spatial-pattern perception exists in the avian telencephalon. Whether the caudal entopallium is directly responsible for motion integration or constitutes an important pre-stage for upstream processing areas remains unknown in the absence of corresponding recordings. But the recipient neurons in the nidopallium have been expected to be involved in higher level motion processing (Wylie & Iwaniuk, 2012). The entopallium projects primarily not only to the ventrolateral mesopallium (MVL) but also to the nidopallium (Krützfeldt & Wild, 2004). Our findings of direction-selectivity with moving dynamic random-dot stimuli suggest that motion integration is solved at the level of the NCL. Such perceptually correlated motion signals could be easily combined with information about other visual attributes, such as shape and colour, or even other modalities, to give rise to a coherent percept of complex moving objects.

Neuronal speed tuning

About a fifth of NCL cells were speed-selective, with half of these neurons acting as high-pass filters and preferring the fastest shown speed of 32 dva/s (and possibly even higher speeds). The broad range of preferred speeds in NCL neurons reflects the speed preferences of the two visual input structures, the entopallium of the tectofugal pathway and the visual Wulst of the thalamofugal pathway. Visual cells along the tectofugal pathway prefer moderate to fast speeds of 20–90 dva/s (Luksch *et al.*, 2004; Frost, 2010). Cells of the pigeon entopallium showed broad ranges of bandpass tuned speed filter functions ranging from 16 to 128 dva/s, with an average optimal speed of 55 dva/s (Gu *et al.*, 2002). In contrast, cells of the owl visual Wulst prefer much slower speeds in the range of 0.5–16 deg/s (Pinto & Baron, 2009). NCL seems to combine these two speed processing streams.

Lack of motion selectivity during the delay period

Few NCL neurons (7.5%) responded to specific motion directions during the delay period. This was the case both over a stationary long as well as several short analysis windows slid over the delay period. This proportion of delay-selective neurons was low compared to our previous results. In a similar DMS task with colourful clipart images, we found that almost 20% of NCL neurons were selective during the delay period (Veit *et al.*, 2014). During a visual association learning task, 27% of NCL neurons showed selective activity to familiar sample images during the delay period. Many more NCL neurons (65% of the total sample) showed association-selective delay activity during a cross-modal delayed association task (Moll & Nieder, 2015). Collectively, this comparison suggests that NCL neurons are particularly engaged during cognitively demanding tasks with complex stimuli.

Neuronal correlates of behavioural performance

As shown by lesion studies in pigeons, the avian NCL seems to be causally involved in mastering delayed response tasks (Mogensen & Divac, 1993; Diekamp *et al.*, 2002). Our data suggest a role of the NCL in judging global motion stimuli. When the crows chose the wrong motion direction, the encoding of the motion direction by the population of selective neurons was drastically reduced in error trials. This is in agreement with our previous findings for delayed response tasks: whenever the crows make errors, activity of selective NCL neurons is reduced and thus predictive of behavioural success (Veit & Nieder, 2013; Veit *et al.*, 2014, 2015a,b; Moll & Nieder, 2015). This suggests that sensory representations of NCL neurons are relevant to the birds' behaviour on a trial-by-trial basis.

Similar correlations of neuronal activity with behavioural performance have been regularly reported for primate PFC neurons. During a motion direction discrimination task, direction-selectivity of PFC cells during the sample phase were significantly diminished on error trials (Zaksas & Pasternak, 2006). In addition, Hussar & Pasternak (2009) found that the selectivity for stimulus direction in the PFC was strongly modulated by task demands.

Comparison with primate prefrontal cortex

Both the anatomical connections and the neuronal response properties of the NCL are reminiscent of the frontal association areas in mammals, which is why the NCL is considered to be the avian functional analogue of the primate prefrontal cortex (PFC; Güntürkün, 2005). However, even though the PFC operates at the apex of the cortical hierarchy and is responsible for executive control functions (Miller & Cohen, 2001), it can represent surprisingly basic sensory information, such as vibrotactile stimuli (Romo *et al.*, 1999) or visual motion information (Zaksas & Pasternak, 2006). In primates, both the dorsal (parietal), most notably motion processing area MT, and the ventral (temporal) visual streams feed into the dorsolateral PFC, providing motion signals to be processed for goal-directed behaviour (reviewed by Pasternak *et al.*, 2003). Zaksas & Pasternak (2006) found that about 20% of the cells recorded in PFC had direction-selective responses, a proportion that mirrors our NCL findings. With an average preferred-anti-preferred selectivity index of 0.45 during the sample period, PFC neurons showed stronger direction modulation (Zaksas & Pasternak, 2006) compared to NCL cells. These motion direction signals in PFC first appeared 113 ms after motion onset (Zaksas & Pasternak, 2006), which was also similar to the median response latency of 112 ms found in this study

for NCL cells. With 19% of the selective neurons, speed tuning was less pronounced in the corvid NCL compared to primate PFC. During a delayed speed comparison task, Hussar & Pasternak (2013) found that 63% of PFC neurons were speed-selective during the sample phase. However, in this experiment, speed was task-relevant. Thus, visual motion signals during stimulus presentation are encoded by a relatively high proportion of neurons both in the primate PFC and the corvid NCL, and with similar characteristics.

Thus, both PFC and NCL, even though operating at the apex of the telencephalic hierarchy, are still involved in processing basic task-relevant sensory parameters, such as motion direction. We think the NCL, as control or selection stage of behaviourally meaningful information, just as the PFC of primates, requires sensory representations to exert top-down influence over information being processed in sensory areas, and to guide goal-directed behaviour based on sensory input (Veit & Nieder, 2013; Lengersdorf *et al.*, 2014).

Acknowledgements

This work was supported by a DFG grant NI 618/6-1 to A.N.

References

Baron, J., Pinto, L., Dias, M.O., Lima, B. & Neuenschwander, S. (2007) Directional responses of visual wulst neurones to grating and plaid patterns in the awake owl. *Eur. J. Neurosci.*, **26**, 1950–1968.

Benowitz, L.I. & Karten, H.J. (1976) Organization of the tectofugal visual pathway in the pigeon: a retrograde transport study. *J. Comp. Neurol.*, **167**, 503–520.

Bischof, W.E., Reid, S.L., Wylie, D.R.W. & Spetch, M.L. (1999) Perception of coherent motion in random dot displays by pigeons and humans. *Percept. Psychophys.*, **61**, 1089–1101.

Capsius, B. & Leppelsack, H.-J. (1996) Influence of urethane anesthesia on neural processing in the auditory cortex analogue of a songbird. *Hearing Res.*, **96**, 59–70.

Diekamp, B., Gagliardo, A. & Güntürkün, O. (2002) Nonspatial and subdivision-specific working memory deficits after selective lesions of the avian prefrontal cortex. *J. Neurosci.*, **22**, 9573–9580.

Ditz, H.M. & Nieder, A. (2015) Neurons selective to the number of visual items in the corvid songbird endbrain. *Proc. Natl. Acad. Sci. USA*, **112**, 7827–7832.

Ditz, H.M. & Nieder, A. (2016) Numerosity representations in crows obey the Weber-Fechner law. *Proc. Biol. Sci.*, **283**, 20160083.

Downing, C.J. & Movshon, J.A. (1989) Spatial and temporal summation in the detection of motion in stochastic random dot displays. *Invest. Ophth. Vis. Sci.*, **30**, 72–86.

Engelage, J. & Bischof, H.-J. (1996) Single-cell responses in the ectostriatum of the zebra finch. *J. Comp. Physiol. A.*, **179**, 785–795.

Frost, B.J. (2010) A taxonomy of different forms of visual motion detection and their underlying neural mechanisms. *Brain Behav. Evolut.*, **75**, 218–235.

Frost, B.J. & DiFranco, D.E. (1976) Motion characteristics of single units in the pigeon optic tectum. *Vision Res.*, **16**, 1229–1234.

Frost, B.J. & Nakayama, K. (1983) Single visual neurons code opposing motion independent of direction. *Science*, **220**, 744–745.

Frost, B.J., Cavanagh, P. & Morgan, B. (1988) Deep tectal cells in pigeons respond to kinematograms. *J. Comp. Physiol.*, **162**, 639–647.

George, I., Vernier, B., Richard, J.-P., Hausberger, M. & Cousillas, H. (2004) Hemispheric specialization in the primary auditory area of awake and anesthetized starlings (*Sturnus vulgaris*). *Behav. Neurosci.*, **118**, 597–610.

Gu, Y., Wang, Y., Zhang, T. & Wang, S.-R. (2002) Stimulus size selectivity and receptive field organization of ectostriatal neurons in the pigeon. *J. Comp. Physiol. A.*, **188**, 173–178.

Güntürkün, O. (2005) The avian "prefrontal cortex" and cognition. *Curr. Opin. Neurobiol.*, **15**, 686–693.

Hodos, W., Smith, L. & Bonbright, J.C. (1975) Detection of the velocity of movement of visual stimuli by pigeons. *J. Exp. Anal. Behav.*, **25**, 143–156.

Hoffmann, A., Rüttler, V. & Nieder, A. (2011) Ontogeny of object permanence and object tracking in the carrion crow, Corvus corone. *Anim. Behav.*, **82**, 359–367.

Hussar, C.R. & Pasternak, T. (2009) Flexibility of sensory representations in prefrontal cortex depends on cell type. *Neuron*, **64**, 730–743.

Hussar, C.R. & Pasternak, T. (2013) Common rules guide comparisons of speed and direction of motion in the dorsolateral prefrontal cortex. *J. Neurosci.*, **33**, 972–986.

Karten, H.J. (1969) The organization of the avian telencephalon and some speculations on the phylogeny of the amniote telencephalon. *Ann. NY. Acad. Sci.*, **167**, 164–179.

Karten, H.J. & Hodos, W. (1967) *Stereotaxic Atlas of the Brain of the Pigeon (*Columba livia*).* The Johns Hopkins Press, Baltimore.

Karten, H.J. & Shimizu, T. (1989) The origins of neocortex: connections and lamination as distinct events in evolution. *J. Cognitive Neurosci.*, **1**, 291–301.

Kröner, S. & Güntürkün, O. (1999) Afferent and efferent connections of the caudolateral neostriatum in the pigeon (*Columba livia*): a retro- and anterograde pathway tracing study. *J. Comp. Neurol.*, **407**, 228–260.

Krützfeldt, N.O.E. & Wild, J.M. (2004) Definition and connections of the entopallium in the zebra finch (*Taeniopygia guttata*). *J. Comp. Neurol.*, **468**, 452–465.

Lengersdorf, D., Pusch, R., Güntürkün, O. & Stüttgen, M.C. (2014) Neurons in the pigeon nidopallium caudolaterale signal the selection and execution of perceptual decisions. *Eur. J. Neurosci.*, **40**, 3316–3327.

Luksch, H., Khanbabaie, R. & Wessel, R. (2004) Synaptic dynamics mediate sensitivity to motion independent of stimulus details. *Nat. Neurosci.*, **7**, 380–388.

Martinoya, C., Rivaud, S. & Bloch, S. (1983) Comparing frontal and lateral viewing in the pigeon. II. Velocity thresholds for movement discrimination. *Behav. Brain Res.*, **8**, 375–385.

Miller, E.K. & Cohen, J.D. (2001) An integrative theory of prefrontal cortex function. *Annu. Rev. Neurosci.*, **24**, 167–202.

Mogensen, J. & Divac, I. (1993) Behavioural effects of ablation of the pigeon-equivalent of the mammalian prefrontal cortex. *Behav. Brain Res.*, **55**, 101–107.

Moll, F.W. & Nieder, A. (2015) Cross-modal associative mnemonic signals in crow endbrain neurons. *Curr. Biol.*, **25**, 2196–2201.

Mulvanny, P. (1978) Velocity discrimination by pigeons. *Vision Res.*, **18**, 531–536.

Ng, B.S.W., Grabska-Barwińska, A., Güntürkün, O. & Jancke, D. (2010) Dominant vertical orientation processing without clustered maps: early visual brain dynamics imaged with voltage-sensitive dye in the pigeon visual wulst. *J. Neurosci.*, **30**, 6713–6725.

Nguyen, A.P., Spetch, M.L., Crowder, N.A., Winship, I.R., Hurd, P.L. & Wylie, D.R.W. (2004) A dissociation of motion and spatial-pattern vision in the avian telencephalon: implications for the evolution of "visual streams". *J. Neurosci.*, **24**, 4962–4970.

Nieder, A. (2016) The neuronal code for number. *Nat. Rev. Neurosci.*, **17**, 366–382.

Nieder, A. & Wagner, H. (1999) Perception and neuronal coding of subjective contours in the owl. *Nat. Neurosci.*, **2**, 660–663.

Nieder, A. & Wagner, H. (2000) Horizontal-disparity tuning of neurons in the visual forebrain of the behaving barn owl. *J. Neurophysiol.*, **83**, 2967–2979.

Nieder, A. & Wagner, H. (2001a) Hierarchical processing of horizontal disparity information in the visual forebrain of behaving owls. *J. Neurosci.*, **21**, 4514–4522.

Nieder, A. & Wagner, H. (2001b) Encoding of both vertical and horizontal disparity in random-dot stereograms by Wulst neurons of awake barn owls. *Visual Neurosci.*, **18**, 541–547.

Parker, A.J. & Newsome, W.T. (1998) Sense and the single neuron: probing the Physiology of Perception. *Annu. Rev. Neurosci.*, **21**, 227–277.

Pasternak, T., Bisley, J.W. & Calkins, D. (2003) Visual processing in the primate brain. In Gallagher, M. & Nelson, R.J. (Eds), *Biological Psychology Handbook of Psychology*. John Wiley & Sons Inc. New York, pp. 139–185.

Pettigrew, J.D. (1979) Binocular visual processing in the owl's telencephalon. *P. Roy. Soc. Lond. B Bio.*, **204**, 435–454.

Pinto, L. & Baron, J. (2009) Spatiotemporal frequency and speed tuning in the owl visual wulst. *Eur. J. Neurosci.*, **30**, 1251–1268.

Romo, R., Brody, C.D., Hernández, A. & Lemus, L. (1999) Neuronal correlates of parametric working memory in the prefrontal cortex. *Nature*, **399**, 470–473.

Schmidt, M.F. & Konishi, M. (1998) Gating of auditory responses in the vocal control system of awake songbirds. *Nat. Neurosci.*, **1**, 513–518.

Shimizu, T. & Bowers, A.N. (1999) Visual circuits of the avian telencephalon: evolutionary implications. *Behav. Brain Res.*, **98**, 183–191.
Sun, H. & Frost, B.J. (1998) Computation of different optical variables of looming objects in pigeon nucleus rotundus neurons. *Nat. Neurosci.*, **1**, 296–303.
Veit, L. & Nieder, A. (2013) Abstract rule neurons in the endbrain support intelligent behaviour in corvid songbirds. *Nat. Commun.*, **4**, 2878.
Veit, L., Hartmann, K. & Nieder, A. (2014) Neuronal correlates of visual working memory in the corvid endbrain. *J. Neurosci.*, **34**, 7778–7786.
Veit, L., Hartmann, K. & Nieder, A. (2015a) Spatially tuned neurons in corvid nidopallium caudolaterale signal target position during visual search. *Cereb Cortex*, doi: 10.1093/cercor/bhv299. [Epub ahead of print].
Veit, L., Pidpruzhnykova, G. & Nieder, A. (2015b) Associative learning rapidly establishes neuronal representations of upcoming behavioral choices in crows. *Proc. Natl. Acad. Sci. USA*, **112**, 15208–15213.
Wagner, H. & Frost, B. (1994) Binocular responses of neurons in the barn owl's visual Wulst. *J. Comp. Physiol. A.*, **174**, 661–670.
Wang, Y. & Frost, B.J. (1992) Time to collision is signalled by neurons in the nucleus rotundus of pigeons. *Nature*, **356**, 236–238.
Wang, Y.C., Jiang, S. & Frost, B.J. (1993) Visual processing in pigeon nucleus rotundus: luminance, color, motion, and looming subdivisions. *Visual Neurosci.*, **10**, 21–30.
Williams, D.W. & Sekuler, R. (1984) Coherent global motion percepts from stochastic local motions. *Vision Res.*, **24**, 55–62.
Wylie, D.R.W. & Iwaniuk, A.N. (2012) Neural mechanisms of motion detection in birds. In Lazareva, O.F., Shimizu, T. & Wasserman, E.A. (Eds), *Comparative Behavior, Biology, and Evolution of Vision, How Animals See the World*. Oxford University Press, New York, pp. 289–318.
Wylie, D.R., Gutiérrez-Ibáñez, C. & Iwaniuk, A.N. (2015) Integrating brain, behavior, and phylogeny to understand the evolution of sensory systems in birds. *Front. Neurosci.*, **9**, 281.
Xiao, Q. & Frost, B.J. (2009) Looming responses of telencephalic neurons in the pigeon are modulated by optic flow. *Brain Res.*, **1305**, 40–46.
Zaksas, D. & Pasternak, T. (2006) Directional signals in the prefrontal cortex and in area MT during a working memory for visual motion task. *J. Neurosci.*, **26**, 11726–11742.